


# Mitochondrial Complex 1, Sigma 1, and Synaptic Vesicle 2A in Early Drug-Naive Parkinson's Disease

Heather Wilson, MSc,<sup>1,2</sup>  Gennaro Pagano, PhD,<sup>2</sup>  Edoardo Rosario de Natale, PhD,<sup>1,2</sup> Ayla Mansur, MSc,<sup>3,4</sup> Silvia Paola Caminiti, PhD,<sup>2</sup> Sotirios Polychronis, MSc,<sup>2</sup> Lefkos T. Middleton, PhD,<sup>5,6,7</sup> Geraint Price, PhD,<sup>5,7</sup> Karl F. Schmidt, PhD,<sup>8</sup> Roger N. Gunn, PhD,<sup>3,4,7</sup> Eugenii A. Rabiner, FCPSych SA,<sup>3,7,9</sup> and Marios Politis, PhD<sup>1,2,7\*</sup>

<sup>1</sup>Neurodegeneration Imaging Group, University of Exeter Medical School, London, UK

<sup>2</sup>Neurodegeneration Imaging Group, Institute of Psychiatry, Psychology and Neuroscience, King's College London, UK

<sup>3</sup>Invicro, Centre for Imaging Sciences, Hammersmith Hospital, London, UK

<sup>4</sup>Division of Brain Sciences, Department of Medicine, Imperial College London, UK

<sup>5</sup>School of Public Health, Imperial College London, UK

<sup>6</sup>Public Health Directorate, Imperial College NHS Healthcare Trust, London, UK

<sup>7</sup>MINDMAPS Consortium, London, UK

<sup>8</sup>Celgene, Cambridge, Massachusetts, USA

<sup>9</sup>Department of Neuroimaging, Institute of Psychiatry, Psychology and Neuroscience, King's College London, London, UK

**ABSTRACT: Background:** Dysfunction of mitochondrial energy generation may contribute to neurodegeneration, leading to synaptic loss in Parkinson's disease (PD). The objective of this study was to find cross-sectional and longitudinal changes in PET markers of synaptic vesicle protein 2A, sigma 1 receptor, and mitochondrial complex 1 in drug-naive PD patients.

**Methods:** Twelve early drug-naive PD patients and 16 healthy controls underwent a 3-Tesla MRI and PET imaging to quantify volume of distribution of [<sup>11</sup>C]UCB-J, [<sup>11</sup>C]SA-4503, and [<sup>18</sup>F]BCPP-EF for synaptic vesicle protein 2A, sigma 1 receptor, and mitochondrial complex 1, respectively. Nine PD patients completed approximately 1-year follow-up assessments.

**Results:** Reduced [<sup>11</sup>C]UCB-J volume of distribution in the caudate, putamen, thalamus, brain stem, and dorsal raphe and across cortical regions was observed in drug-naive PD patients compared with healthy controls. [<sup>11</sup>C]UCB-J volume of distribution was reduced in the locus coeruleus and substantia nigra but did not reach statistical significance. No significant differences were found in [<sup>11</sup>C]SA-4503 and

[<sup>18</sup>F]BCPP-EF volume of distribution in PD compared with healthy controls. Lower brain stem [<sup>11</sup>C]UCB-J volume of distribution correlated with Movement Disorder Society Unified Parkinson's Disease Rating Scale part III and total scores. No significant longitudinal changes were identified in PD patients at follow-up compared with baseline.

**Conclusions:** Our findings represent the first in vivo evidence of mitochondrial, endoplasmic reticulum, and synaptic dysfunction in drug-naive PD patients. Synaptic dysfunction likely occurs early in disease pathophysiology and has relevance to symptomatology. Mitochondrial complex 1 and sigma 1 receptor pathology warrants further investigations in PD. Studies in larger cohorts with longer follow-up will determine the validity of these PET markers to track disease progression. © 2020 The Authors. *Movement Disorders* published by Wiley Periodicals, Inc. on behalf of International Parkinson and Movement Disorder Society.

**Key Words:** mitochondria; molecular biomarkers; Parkinson's disease; positron emission tomography; synaptic vesicle protein

This is an open access article under the terms of the Creative Commons Attribution License, which permits use, distribution and reproduction in any medium, provided the original work is properly cited.

\*Correspondence to: Prof. Marios Politis; Neurodegeneration Imaging Group, University of Exeter Medical School, London, UK; E-mail: m.politis@exeter.ac.uk

Heather Wilson and Gennaro Pagano contributed equally to this article.

**Relevant conflicts of interest/financial disclosures:** No authors report any conflicts of interest relevant to this article. A.M., E.A.R., and R.N.G. are employees of Invicro LLC; G.P. is currently a full-time employee of F. Hoffmann-La Roche Ltd, but at the time of study design

and conduct he was a full-time employee of King's College London, with no other disclosures; R.N.G. is a consultant for AbbVie, Biogen, and Cerveau. K.F.S. is employed by Celgene Corporation. No potential conflicts of interest relevant to this article exist.

**Funding agencies:** The project was funded by the MIND-MAPS consortium.

**Received:** 7 January 2020; **Revised:** 27 March 2020; **Accepted:** 30 March 2020

**Published online 29 April 2020 in Wiley Online Library (wileyonlinelibrary.com). DOI: 10.1002/mds.28064**

Preclinical evidence suggests that the mechanisms underlying the pathophysiology of Parkinson's disease (PD) involves mitochondrial,<sup>1</sup> endoplasmic reticulum (ER),<sup>2</sup> and synaptic<sup>3</sup> function. Synaptic vesicle protein 2A (SV2A) is a transmembrane protein widely expressed in presynaptic terminals throughout the brain, where it regulates neurotransmission.<sup>4,5</sup> Neurons lacking SV2A demonstrate impaired ability of vesicles to fuse with the plasma membrane.<sup>6</sup> There are several lines of evidence suggesting that accumulation of  $\alpha$ -synuclein in presynaptic terminals impairs synaptic proteins, synaptic plasticity, and neurotransmission and subsequently induces axonal damage and impairment of intracellular trafficking.<sup>7-16</sup>

Sigma 1 receptor ( $\sigma$ 1R) is a chaperone protein residing at the mitochondrion-associated endoplasmic reticulum membrane, where it modulates calcium influx into the mitochondrion from the ER and is thought to play a role in regulating the activity of potassium channels.<sup>17</sup> Activation of  $\sigma$ 1Rs stimulates neuromodulation and neuroprotection.<sup>18</sup> The  $\sigma$ 1R facilitates the proper folding of newly synthesized proteins, but also prevents accumulation of misfolded proteins, suggesting that  $\sigma$ 1R plays a key role in cellular survival, and its upregulation may be neuroprotective, given that it may prevent the accumulation of abnormal proteins.<sup>19,20</sup> Furthermore,  $\sigma$ 1R stimulates striatal dopamine synthesis in rats and has been hypothesized to play a role in the pathophysiology of PD.<sup>21</sup>

Mitochondrial complex 1 (MC1) is the first enzyme complex in the electron transfer chain, having a critical role in oxidative phosphorylation in mitochondria.<sup>22</sup> A common finding in animal models of PD as well as in brain tissue of patients with sporadic and familial forms of PD is the presence of histopathological evidence of progressive mitochondrial dysfunction.<sup>23,24</sup> Mitochondrial dysfunction is mainly characterized by the generation of reactive oxygen species, decreased MC1 enzyme activity, adenosine triphosphate depletion, and caspase-3 activation. Marked decreases in MC1 activity and reduced mitochondrial DNA levels were widely found in postmortem PD brain samples.<sup>25-28</sup>

The development of selective PET radioligands [<sup>11</sup>C]UCB-J for SV2A,<sup>29</sup> [<sup>11</sup>C]SA-4503 for  $\sigma$ 1R,<sup>30</sup> and [<sup>18</sup>F]BCPP-EF for MC1,<sup>31,32</sup> allows for the *in vivo* investigation of presynaptic terminals and the mitochondrial/ER complex in neurodegenerative disorders. Here, we performed cross-sectional and longitudinal measurements using these 3 PET radioligands, 3-Tesla MRI, and a battery of clinical assessments in a cohort of early drug-naive PD patients.

## Methods

### Participant Demographics

Twenty-eight participants were recruited, 12 with idiopathic PD from specialist movement disorders clinics at

King's College Hospital and 16 age-matched healthy controls through public advertisement. PD patients were recruited according to the following inclusion criteria: (1) PD diagnosed according to the Queen Square Brain Bank criteria; (2) duration of PD symptoms  $\leq$ 24 months; (3) naive to PD treatment at baseline; (4) did not fulfill the diagnostic criteria for PD mild cognitive impairment,<sup>33</sup> dementia,<sup>34</sup> or depression<sup>35</sup>; (5) no history of other neurological or psychiatric disorders; and (6) no contraindication to MRI. Healthy controls had no history of neurological or psychiatric disorders. None of the participants were on medications or supplements with known affinity for the SV2A,  $\sigma$ 1R, or MC1, including metformin, neuroactive steroids (such as dehydroepiandrosterone, progesterone, pregnenolone, testosterone, and deoxycorticosterone), haloperidol, fluvoxamine, donepezil, levetiracetam, and bevetiracetam.

All participants were successfully screened to undertake PET and MRI scanning under scanning safety criteria (<http://www.mrisafety.com>; <https://www.gov.uk/government/publications/arsac-notes-for-guidance>). The study was approved by the institutional review board and the research ethics committee. Permission to use radioactive substances was obtained by the Administration of Radioactive Substances Advisory Committee, Department of Health and Social Care, United Kingdom. Written informed consent was obtained from all study participants in accordance with the Declaration of Helsinki.

### Clinical Assessments

Clinical assessments were performed at the NIHR King's Wellcome Clinical Research Facility (London, UK). Motor symptom severity was assessed using the Movement Disorder Society Unified Parkinson's Disease Rating Scale (MDS-UPDRS) part III and staged with the Hoehn and Yahr (H&Y) scale. MDS-UPDRS total scores were used to assess global disease burden. Mini-Mental Status Examination and Montreal Cognitive Assessment were used to assess global cognitive status. Nonmotor symptoms were assessed with the Non-Motor Symptoms Scale (NMSS), the Parkinson's Disease Sleep Scale for sleep disturbances, and the Beck Depression Inventory second edition for depression.

### Longitudinal Follow-up

Eight PD patients completed longitudinal [<sup>11</sup>C]UCB-J, [<sup>11</sup>C]SA-4503, and [<sup>18</sup>F]BCPP-EF PET scans, MRI and clinical assessments at a mean follow-up period of  $11 \pm 1.3$  months (range, 10–14 months). A ninth PD patient completed only [<sup>11</sup>C]SA-4503 and [<sup>18</sup>F]BCPP-EF PET and clinical assessments at follow-up. At follow-up, all PD patients remained drug naive except for 1 patient who was started on levodopa treatment (daily levodopa-equivalent dose of 150 mg) 6 months before the follow-up

assessments. Motor assessments were performed OFF medication after overnight withdrawal of dopaminergic medication for this 1 PD patient.

### Scanning Procedures

All participants were underwent 3 PET scans with [ $^{11}\text{C}$ ]UCB-J, [ $^{11}\text{C}$ ]SA-4503, and [ $^{18}\text{F}$ ]BCPP-EF and one 3-Tesla MRI at Invicro (London, UK) on a Siemens Biograph Hi-Rez 6 or Biograph TruePoint 6 PET-CT scanner (Siemens Healthcare, Erlangen, Germany), and Siemens 3-Tesla Magnetom Trio MRI scanner with a 32-channel head coil (Siemens Healthcare, Erlangen, Germany), respectively. [ $^{11}\text{C}$ ]UCB-J ( $235 \pm 42.9$  MBq), [ $^{11}\text{C}$ ]SA-4503 ( $252 \pm 36.0$  MBq) and [ $^{18}\text{F}$ ]BCPP-EF ( $90 \pm 5.0$  MBq) were administered intravenously as a slow bolus over 20 seconds. For each subject at baseline and follow-up, [ $^{11}\text{C}$ ]UCB-J PET, [ $^{11}\text{C}$ ]SA-4503 PET, [ $^{18}\text{F}$ ]BCPP-EF PET, and MRI were performed within a period of no more than 16 days. Nonsteroidal anti-inflammatory drugs (such as aspirin, indomethacin, diclofenac, piroxicam, and ibuprofen) were discontinued at least 4 days prior to the [ $^{18}\text{F}$ ]BCPP-EF PET scans.

Dynamic emission PET data were acquired continuously for 90 minutes following the injection of [ $^{11}\text{C}$ ]UCB-J, [ $^{11}\text{C}$ ]SA-4503, and [ $^{18}\text{F}$ ]BCPP-EF and reconstructed into 26 frames ( $8 \times 15$ ,  $3 \times 60$ ,  $5 \times 120$ ,  $5 \times 300$ , and  $5 \times 600$  seconds), using a filtered back-projection algorithm (direct inversion Fourier transform) with a 128 matrix, 2.6 zoom producing images with an isotropic voxel size of  $2 \times 2 \times 2$  mm<sup>3</sup> and smoothed with a transaxial Gaussian filter of 5 mm. All participants underwent arterial sampling and metabolite analysis to enable generation of a parent plasma input function for all 3 tracers, [ $^{11}\text{C}$ ]UCB-J, [ $^{11}\text{C}$ ]SA-4503, and [ $^{18}\text{F}$ ]BCPP-EF.

MRI scans were acquired for the following sequences using a 1 mm<sup>3</sup> voxel size, anteroposterior phase encoding direction, and a symmetric echo. T1-weighted magnetization prepared rapid gradient echo sequence for coregistration with the PET images; fast gray matter T1 inversion recovery (FGATIR<sup>36</sup>) for volumetric quantification of the substantia nigra and neuromelanin-sensitive T1-weighted for delineation of the locus coeruleus. Full acquisition parameters are outlined in the Supplemental Materials.

### imaging Data Analysis

#### MRI-Based Volumetric Analysis

Cortical thickness and deep gray matter nuclei volumetric changes were investigated with FreeSurfer image analysis suite (version 6.0), as previously validated,<sup>37</sup> in healthy controls and PD patients at baseline and follow-up. All individual nuclei volumes were normalized for intracranial volume.<sup>38</sup> To better quantify

volumetric changes, the substantia nigra was manually delineated on the FGATIR sequence,<sup>39</sup> using the Analyze medical imaging software package (version 12.0; Mayo Foundation, Overland Park, Kansas, United States).

#### PET Data Analysis

All PET data analysis was performed as previously described.<sup>40</sup> Briefly, the Molecular Imaging and Kinetic Analysis Toolbox software package (MIAKAT version 4.3.7; <http://www.miakat.org>), implemented in MATLAB (version R2016a; The Mathworks, Natick, MA) was used to carry out image processing and kinetic modeling. MIAKAT combines inhouse code with wrappers for FMRIB Software Library (FSL; version 5.0.9; <http://fsl.fmrib.ox.ac.uk/fsl/fslwiki/>) and Statistical Parametric Mapping (SPM; version 12; <http://www.fil.ion.ucl.ac.uk/spm/>). Individual PET frames were corrected for head motion using frame-by-frame rigid registration using a frame with high signal-to-noise ratio as reference. Plasma input function of unmetabolized radioligand was generated using the continuous blood, discrete blood/plasma samples and metabolite assays. For [ $^{11}\text{C}$ ]UCB-J and [ $^{18}\text{F}$ ]BCPP-EF the arterial input function was obtained by plasma-to-whole blood ratios fitted with a constant fit and a sigmoid fit for parent fraction. For [ $^{11}\text{C}$ ]SA-4503 plasma-to-whole blood ratios were fitted with an exponential approach to constant fit and an exponential plus constant fit for parent fraction. The plasma free fraction ( $f_p$ ) was measured by ultrafiltration in triplicate using an arterial blood sample taken prior to tracer injection as previously described.<sup>40</sup> Where there were differences in  $f_p$ , regional differences in tracer uptake were explored using  $V_T/f_p$  as an outcome measure.

Regional estimates of [ $^{11}\text{C}$ ]SA-4503 and [ $^{18}\text{F}$ ]BCPP-EF volume of distribution ( $V_T$ ) were generated using the graphical model multilinear analysis 1 (MA1<sup>41</sup>;  $t^* = 30$  minutes) with blood volume correction. [ $^{11}\text{C}$ ]SA-4503 and [ $^{18}\text{F}$ ]BCPP-EF parametric  $V_T$  maps were generated with Logan Graphical analysis.<sup>42</sup> Regional estimates of [ $^{11}\text{C}$ ]UCB-J  $V_T$  were generated using the 1-tissue compartmental model (1TC) with blood volume correction and parametric  $V_T$  maps generated using 1TC model.<sup>43</sup> The centrum semiovale has been previously suggested as a white-matter pseudo-reference region for [ $^{11}\text{C}$ ]UCB-J.<sup>44</sup> Therefore, for [ $^{11}\text{C}$ ]UCB-J, a distribution volume ratio minus 1 of the target region and the centrum semiovale (DVR-1) was estimated from the volumes of distribution ( $[V_T^{\text{ROI}}/V_T^{\text{CS}}] - 1$ ).

#### Region-of-Interest-Based Analysis

To facilitate anatomical delineation of regions of interest, PET images were anatomically coregistered and resliced to the corresponding volumetric structural

**TABLE 1.** Clinical characteristics of early drug-naive Parkinson's disease patients at baseline and follow-up

ID	Age (years)	Disease duration (months)	H&Y OFF	MDS-UPDRS total	MDS-UPDRS-III OFF	NMSS	BDI-II	MMSE	MoCA	PDSS
1	59	4	1	9	8	1	2	30	30	145
2	66	1	1	25	17	15	3	30	28	130
3	69	41	1	18	10	2	3	26	28	148
4 BL	49	12	1	23	13	19	1	30	28	108
4 FU	50	26	1	26	15	24	0	30	28	119
5 BL	63	5	1	28	20	30	3	30	30	115
5 FU	64	16	1	35	23	44	0	30	30	101
6 BL	47	33	1	11	8	3	0	30	30	142
6 FU	48	43	1	15	12	5	0	30	30	144
7 BL	63	20	1	16	8	18	3	30	30	141
7 FU	64	31	1	22	14	22	2	29	29	144
8 BL	47	36	1	20	8	21	4	29	28	129
8 FU	48	46	2	22	11	28	7	30	30	128
9 BL	57	24	1	49	28	4	6	30	30	134
9 FU	58	34	2	56	36	7	4	29	30	145
10 BL	77	12	1	25	18	18	3	30	30	133
10 FU	78	24	2	41	28	23	2	27	29	133
11 BL	59	11	1	23	16	3	2	26	28	131
11 FU	60	22	1	28	18	4	1	30	30	143
12 BL	62	24	1	33	15	18	9	30	30	130
12 FU	63	35	1	37	24	20	8	30	30	137
PD baseline (n = 12), mean ± SD	59.8 ± 9.0	18.6 ± 13.2	1 ± 0	23.3 ± 10.6	14.1 ± 6.2	12.7 ± 9.6	3.3 ± 2.3	29.3 ± 1.5	29.2 ± 1.0	132.2 ± 11.7
PD follow-up (n = 9), mean ± SD	59.2 ± 9.7	30.8 ± 9.7	1.3 ± 0.5	31.3 ± 12.4	20.1 ± 8.3	19.7 ± 12.8	2.7 ± 3.0	29.4 ± 1.0	29.6 ± 0.7	132.7 ± 14.8
Within-subject change at follow-up, mean ± SD	—	—	0.3 ± 0.5	6.0 ± 4.1	5.2 ± 3.1	4.8 ± 3.9	-0.8 ± 1.6	0.2 ± 1.1	0.0 ± 1.9	3.4 ± 8.2

H&Y, Hoehn and Yahr; MDS-UPDRS III, Movement Disorder Society-sponsored revision of the Unified Parkinson's Disease Rating Scale part III — Motor; NMSS, Non-Motor Symptoms Scale; BDI-II, Beck Depression Inventory-II; HDRS, Hamilton Depression Rating Scale; MMSE, Mini Mental Status Examination; MoCA, Montreal Cognitive Assessment; PDSS, Parkinson's Disease Sleep Scale; BL, baseline; FU, follow-up.

**TABLE 2.** Cross-sectional analysis of synaptic vesicle protein 2A, sigma 1 receptor, and mitochondrial complex 1 levels in early drug-naive Parkinson's disease patients compared with healthy controls

Radioligand (target)	Cohort	Region of interest													
		FC	PC	TC	OC	INS	HIP	CAU	PUT	THA	BST	Medianraphe	Dorsalraphe	SN	LC
<sup>11</sup> C]JUCB-J Vr (SV2A)	HC (n = 16)	17.7 ± 2.1	18.0 ± 2.3	19.1 ± 1.8	18.2 ± 2.0	20.7 ± 2.0	14.3 ± 1.5	14.2 ± 2.7	22.5 ± 2.1	13.3 ± 2.0	8.5 ± 1.1	8.7 ± 1.0	10.1 ± 1.2	8.6 ± 0.9	9.6 ± 1.0
	PD <sup>a</sup> (n = 11)	15.8 ± 2.2	16.0 ± 2.2	17.4 ± 1.9	16.2 ± 2.0	19.1 ± 2.3	13.2 ± 1.6	12.1 ± 2.6	20.3 ± 2.3	11.8 ± 2.2	7.7 ± 0.9	8.1 ± 0.9	9.2 ± 1.1	8.0 ± 0.9	8.8 ± 1.3
	% change	-10.3%	-11.0%	-9.0%	-11.0%	-7.9%	-7.8%	-15.1%	-9.7%	-11.6%	-9.4%	-6.7%	-9.4%	-6.9%	-8.7%
	<i>P</i>	<b>0.028</b>	<b>0.028</b>	<b>0.028</b>	<b>0.028</b>	<b>0.029</b>	0.051	<b>0.028</b>	<b>0.028</b>	<b>0.028</b>	<b>0.028</b>	0.064	<b>0.028</b>	0.064	0.055
<sup>11</sup> C]SA-4503 Vr (σ1R)	Cohen's <i>d</i>	0.86	0.88	0.92	1.00	0.77	0.71	0.82	0.99	0.74	0.81	0.61	0.83	0.68	0.73
	HC (n = 16)	39.4 ± 8.6	37.4 ± 6.8	39.7 ± 6.5	35.5 ± 6.8	43.8 ± 6.8	37.6 ± 5.7	28.6 ± 7.5	42.5 ± 7.5	35.4 ± 7.1	36.5 ± 6.3	41.4 ± 12.2	35.6 ± 7.6	34.5 ± 7.5	28.3 ± 6.4
	PD (n = 12)	35.4 ± 7.7	34.0 ± 6.3	37.8 ± 7.1	34.3 ± 6.1	42.7 ± 7.9	35.1 ± 6.5	22.9 ± 6.0	40.7 ± 7.4	30.9 ± 8.2	32.9 ± 6.5	36.3 ± 10.6	32.1 ± 8.1	34.4 ± 5.7	28.0 ± 8.3
	% change	-10.0%	-9.1%	-4.7%	-3.4%	-2.3%	-6.5%	-20.1%	-4.2%	-12.8%	-9.9%	-12.4%	-9.9%	-0.4%	-0.8%
<sup>18</sup> F]BCPP-EF Vr (MC1)	<i>P</i>	>0.1	>0.1	>0.1	>0.1	>0.1	>0.1	>0.1	>0.1	>0.1	>0.1	>0.1	>0.1	>0.1	>0.1
	Cohen's <i>d</i>	0.48	0.52	0.27	0.19	0.14	0.40	0.85	0.24	0.59	0.57	0.45	0.45	0.02	0.03
	HC (n = 16)	24.9 ± 4.4	25.9 ± 5.1	24.5 ± 4.1	27.6 ± 4.8	26.3 ± 4.4	21.5 ± 3.7	23.2 ± 5.5	36.0 ± 6.3	25.4 ± 5.1	18.6 ± 3.1	22.4 ± 3.8	22.0 ± 3.3	20.7 ± 3.1	20.3 ± 3.5
	PD (n = 12)	23.0 ± 5.4	24.2 ± 6.0	22.9 ± 4.8	25.2 ± 5.8	24.8 ± 4.9	19.9 ± 4	21.0 ± 6.2	33.3 ± 6.9	22.5 ± 6.0	16.6 ± 3.2	20.7 ± 4.3	19.6 ± 3.9	19.3 ± 4.0	18.4 ± 4.1
PD, Parkinson's disease; HC, healthy control; FL, frontal cortex; PL, parietal cortex; TL, temporal cortex; OL, occipital cortex; INS, insula; HIP, hippocampus; CAU, caudate; PUT, putamen; TH, thalamus; BST, brain stem; SN, substantia nigra; LC, locus coeruleus; MC1, mitochondrial complex 1; SV2A, synaptic vesicle protein 2A; σ1R, sigma 1 receptor.	% change	-7.5%	-6.6%	-6.7%	-8.9%	-5.8%	-7.2%	-9.4%	-7.6%	-11.3%	-10.9%	-7.6%	-10.8%	-6.7%	-9.0%
	<i>P</i>	>0.1	>0.1	>0.1	>0.1	>0.1	>0.1	>0.1	>0.1	>0.1	>0.1	>0.1	>0.1	>0.1	>0.1
	Cohen's <i>d</i>	0.39	0.30	0.37	0.46	0.33	0.40	0.37	0.41	0.52	0.64	0.42	0.66	0.39	0.48
	For [ <sup>11</sup> C]UCB-J analysis, 1 PD patient was excluded as an outlier. All data are presented as mean ± standard deviation, and the level α was set for all comparisons at <i>P</i> < 0.05.														

PD, Parkinson's disease; HC, healthy control; FL, frontal cortex; PL, parietal cortex; TL, temporal cortex; OL, occipital cortex; INS, insula; HIP, hippocampus; CAU, caudate; PUT, putamen; TH, thalamus; BST, brain stem; SN, substantia nigra; LC, locus coeruleus; MC1, mitochondrial complex 1; SV2A, synaptic vesicle protein 2A; σ1R, sigma 1 receptor.

<sup>a</sup>For [<sup>11</sup>C]UCB-J analysis, 1 PD patient was excluded as an outlier. All data are presented as mean ± standard deviation, and the level α was set for all comparisons at *P* < 0.05.

T1-weighted MRI images in SPM. The template brain image and associated Clinical Imaging Centre atlas<sup>39</sup> was then nonlinearly warped to the individual subject's MRI image where the following regions of interest were defined: frontal cortex, insular cortex, temporal cortex, parietal cortex, hippocampus, brain stem, thalamus, caudate, putamen, and substantia nigra. Dorsal and

median raphe nuclei were defined using the Harvard Ascending Arousal Network Atlas.<sup>45</sup> To tailor regions of interest to a subject's individual anatomy, the subject's segmented gray matter was used to mask the regions of interest. Time-activity curves were generated within the gray matter-masked regions of interest. The locus coeruleus was manually delineated on the

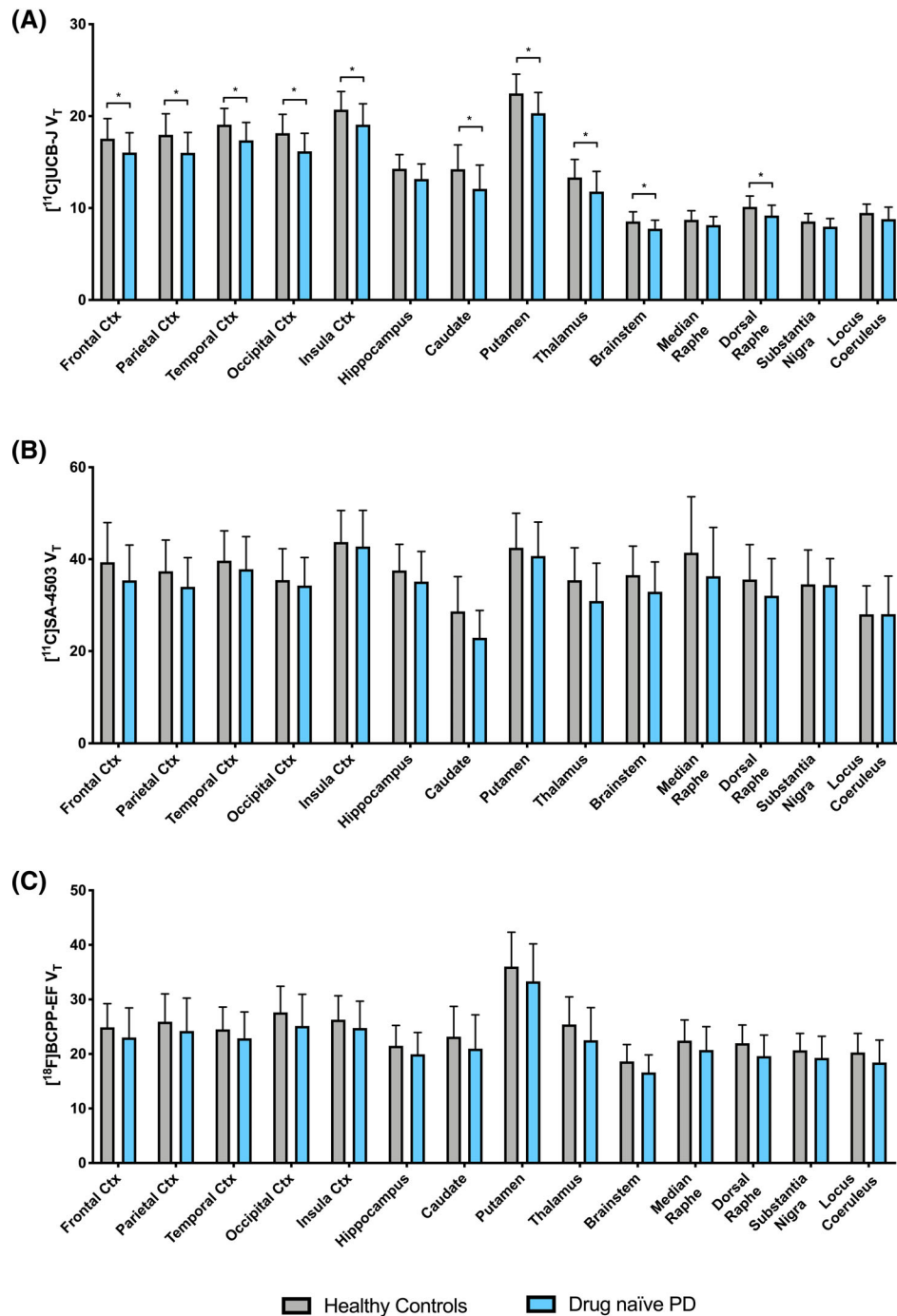


**FIG. 1.** Bar graphs showing cross-sectional analysis of synaptic vesicle protein 2A, sigma 1 receptor and mitochondrial complex 1 in drug-naive Parkinson's disease patients. Regional total distribution volume ( $V_T$ ) in [<sup>11</sup>C]UCB-J (A), [<sup>11</sup>C]SA-4503 (B), and [<sup>18</sup>F]BCPP-EF (C) in drug-naive Parkinson's disease patients compared with healthy controls. \* $P < 0.05$ . [Color figure can be viewed at [wileyonlinelibrary.com](http://wileyonlinelibrary.com)]

neuromelanin-sensitive T1-weighted MRI images using Analyze.

### Statistical Analysis

Statistical analysis and graph illustration were performed with SPSS (version 25; Chicago, IL) and GraphPad Prism (version 7.0c) for Mac OS X, respectively. For all variables, Gaussianity was tested with the Shapiro-Wilk test. We proceeded with parametric tests, as our data were normally distributed. Independent *t* tests were used to assess between-group differences in clinical variables. Multivariate analysis of covariance was used to assess between-group differences in regions of interest for each PET tracer and MRI volumetric data. Although there was no difference in age between groups (Table 1), age was included as a covariate because of a possible age effect on these PET markers.<sup>40,46</sup> *P* values for each variable were calculated following Benjamin-Hochberg correction to control the false discovery rate (FDR).<sup>47</sup> Paired *t* tests were used to assess longitudinal changes in clinical, PET, and MRI variables. The within-subject annual rate of change was calculated as follows: (% change from baseline to follow-up  $\times$  12 months)/between-scan interval (months). We interrogated correlations between PET and clinical data using Pearson's *r*, and we applied Benjamin-Hochberg correction to control the FDR.<sup>47</sup> The relationship between SV2A,  $\sigma$ 1R, and MC1 was investigated at a molecular level in exploratory analysis by interrogating correlations between the regional uptake of each PET tracer within the drug-naïve PD cohort. In this exploratory analysis, correction for multiple comparisons was not applied. We tested for outliers using the ROUT outlier test, based on the FDR, in GraphPad Prism. For longitudinal analysis, follow-up period and change in age were included as covariates. We set the false discovery rate cutoff at 0.05. All data are presented as mean  $\pm$  standard deviation, and the

level  $\alpha$  was set for all comparisons at  $P < 0.05$ , corrected.

## Results

### Clinical Characteristics

Healthy controls had an average age of  $61.0 \pm 12.5$  years and a sex distribution of 8 men and 8 women. There was no difference in age ( $P = 0.71$ ) or sex ( $P = 0.074$ ) between PD patients and healthy controls. PD patients had no significant cognitive impairment, were not depressed, and did not have sleep disturbances (Table 1). At follow-up PD patients showed progression of motor symptoms (within-subject mean change: MDS-UPDRS-III OFF  $5.2 \pm 3.1$ ,  $P = 0.001$ ; H&Y OFF  $0.3 \pm 0.5$ ,  $P = 0.081$ ) and higher burden of nonmotor symptoms (within-subject mean change: NMSS  $4.8 \pm 3.9$ ,  $P = 0.007$ ; Table 1).

### Cross-Sectional Analysis

#### Region-of-Interest-Based [<sup>11</sup>C]UCB-J, [<sup>11</sup>C]SA-4503 and [<sup>18</sup>F]BCPP-EF PET Analysis

Cross-sectional analysis revealed significant loss of [<sup>11</sup>C]UCB-J  $V_T$  in early drug-naïve PD patients compared with healthy controls. Although [<sup>11</sup>C]SA-4503  $V_T$  and [<sup>18</sup>F]BCPP-EF  $V_T$  showed overall reductions in PD, there were no statistically significant differences in the regions of interest (Table 2, Fig. 1). The  $f_p$  was not different for any of the 3 tracers between PD patients and healthy controls (Table S1).

Early drug-naïve PD patients demonstrated significantly reduced [<sup>11</sup>C]UCB-J  $V_T$  in the striatum, thalamus, brain stem, and dorsal raphe, as well as across cortical regions compared with healthy controls (Table 2, Fig. 1A). [<sup>11</sup>C]UCB-J  $V_T$  showed reductions in the locus coeruleus, substantia nigra, hippocampus, and median raphe in PD patients; however, these did

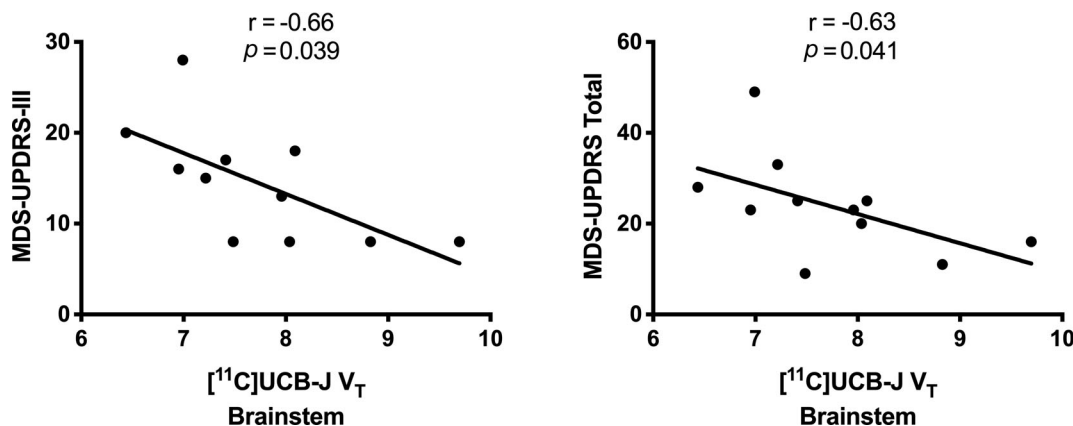


**FIG. 2.** Correlations between [<sup>11</sup>C]UCB-J  $V_T$  with clinical markers of disease burden in drug-naïve Parkinson's disease patients. Loss of [<sup>11</sup>C]UCB-J  $V_T$  in the brain stem correlated with higher scores on MDS-UPDRS part III, as a measure of motor symptom severity, and higher MDS-UPDRS Total score, as a measure of global symptom burden in early drug-naïve Parkinson's disease patients.

**TABLE 3.** Longitudinal analysis of synaptic vesicle protein 2A, sigma 1 receptor, and mitochondrial complex 1 levels in early Parkinson's disease patients

Radioligand (target)	Cohort	Region of interest													
		FC	PC	TC	OC	INS	HIP	CAU	PUT	THA	BST	Medianraphe	Dorsalraphe	SN	LC
<sup>11</sup> CJUCB-JVt (SV2A)	PD BL (n = 7)	15.9 ± 1.6	16.4 ± 1.3	17.4 ± 1.5	16.5 ± 1.4	19.2 ± 1.8	13.2 ± 1.4	12.7 ± 1.9	20.4 ± 1.9	12.3 ± 1.4	7.7 ± 0.7	8.1 ± 0.7	9.0 ± 0.9	7.8 ± 0.8	8.6 ± 0.7
	PD FU <sup>a</sup> (n = 7)	16.1 ± 1.4	16.2 ± 0.9	17.8 ± 1.2	16.6 ± 0.6	19.5 ± 1.3	13.1 ± 1.1	12.5 ± 2.0	20.6 ± 1.6	12.3 ± 1.1	7.6 ± 0.4	8.1 ± 1.3	9.0 ± 1.9	7.7 ± 0.7	8.7 ± 0.6
	Within-subject annualized % change	1.1%	-0.9%	3.5%	0.8%	1.7%	-0.8%	-2.3%	1.4%	1.4%	0.02%	-1.3%	0.53%	-0.03%	1.6%
<sup>11</sup> CJSA-4503 Vt (σ1R)	PD BL (n = 9)	>0.1	>0.1	>0.1	>0.1	>0.1	>0.1	>0.1	>0.1	>0.1	>0.1	>0.1	>0.1	>0.1	>0.1
	PD FU (n = 9)	36.2 ± 7.2	34.3 ± 6.62	38.0 ± 7.2	34.5 ± 6.5	43.5 ± 8.3	36.3 ± 6.6	24.1 ± 5.9	41.1 ± 7.6	32.9 ± 7.8	32.8 ± 6.39	38.2 ± 11.6	33.4 ± 9.0	33.7 ± 5.5	30.0 ± 8.6
	Within-subject annualized % change	7.1%	5.7%	9.5%	6.8%	6.1%	6.1%	15.4%	9.8%	10.1%	13.8%	-4.0%	-1.7%	3.6%	-4.9%
<sup>18</sup> FJBCPP-EF Vt (MC1)	PD BL (n = 9)	>0.1	>0.1	>0.1	>0.1	>0.1	>0.1	>0.1	>0.1	>0.1	>0.1	>0.1	>0.1	>0.1	>0.1
	PD FU (n = 9)	22.8 ± 6.1	24.2 ± 6.9	22.6 ± 5.6	25.5 ± 6.7	24.8 ± 5.7	19.9 ± 4.7	21.4 ± 7.0	33.1 ± 7.9	23.1 ± 6.7	16.3 ± 3.7	19.8 ± 4.6	19.2 ± 4.4	18.4 ± 4.2	18.47 ± 5.0
	Within-subject annualized % change	8.9%	8.1%	11.3%	10.7%	9.4%	10.3%	8.4%	12.1%	9.4%	10.4%	7.3%	11.4%	9.7%	7.4%
P	>0.1	>0.1	>0.1	>0.1	>0.1	>0.1	>0.1	0.082	>0.1	>0.1	>0.1	>0.1	>0.1	>0.1	

PD, Parkinson's disease; BL, baseline; FU, follow-up; FL, frontal cortex; PL, parietal cortex; TL, temporal cortex; OL, occipital cortex; INS, insula; HIP, hippocampus; CAU, caudate; PUT, putamen; THA, thalamus; BST, brain stem; SN, substantia nigra; LC, locus coeruleus; MC1, mitochondrial complex 1; SV2A, synaptic vesicle protein 2A; σ1R, sigma 1 receptor.  
<sup>a</sup>For [<sup>11</sup>C]UCB-J analysis, 1 PD patient was excluded as an outlier. All data are presented as mean ± standard deviation, and the level α was set for all comparisons at P < 0.05.



not reach statistical significance (Table 2). One PD patient at baseline and 1 patient at follow-up, identified as outliers, were excluded from [ $^{11}\text{C}$ ]UCB-J PET analysis. [ $^{11}\text{C}$ ]UCB-J DVR-1 analysis revealed reductions within the striatum, thalamus, brain stem, dorsal raphe, and across cortical regions; however, these did not survive FDR correction for multiple comparisons (Table S2).

### Correlations

In early drug-naïve PD patients, lower [ $^{11}\text{C}$ ]UCB-J  $V_T$  in the brain stem correlated with higher MDS-UPDRS part III ( $r = -0.66$ ;  $P = 0.039$ ) and higher MDS-UPDRS total score ( $r = -0.63$ ;  $P = 0.041$ ; Fig. 2A).

Exploratory analysis revealed within the caudate, lower [ $^{11}\text{C}$ ]UCB-J  $V_T$  correlated with both lower [ $^{11}\text{C}$ ]SA-4503  $V_T$  ( $r = 0.86$ ;  $P = 0.001$ ) and lower [ $^{18}\text{F}$ ]BCPP-EF  $V_T$  ( $r = 0.75$ ;  $P = 0.008$ ; Fig. S1A). Within the brain stem, lower [ $^{11}\text{C}$ ]UCB-J  $V_T$  correlated with lower [ $^{18}\text{F}$ ]BCPP-EF  $V_T$  ( $r = 0.68$ ;  $P = 0.021$ ; Fig. S1B); and within the dorsal raphe, lower [ $^{11}\text{C}$ ]UCB-J  $V_T$  correlated with lower [ $^{18}\text{F}$ ]BCPP-EF  $V_T$  ( $r = 0.62$ ;  $P = 0.031$ ; Fig. S1C). Moreover, within the substantia nigra, lower [ $^{11}\text{C}$ ]UCB-J  $V_T$  correlated with lower [ $^{18}\text{F}$ ]BCPP-EF  $V_T$  ( $r = 0.71$ ;  $P = 0.015$ ; Fig. S1D).

### Longitudinal Analysis

#### Longitudinal Region-of-Interest-Based [ $^{11}\text{C}$ ]UCB-J, [ $^{11}\text{C}$ ]SA-4503, and [ $^{18}\text{F}$ ]BCPP-EF PET Analysis

No significant longitudinal changes were identified in [ $^{11}\text{C}$ ]UCB-J  $V_T$ , [ $^{11}\text{C}$ ]UCB-J DVR-1, [ $^{11}\text{C}$ ]SA-4503  $V_T$ , or [ $^{18}\text{F}$ ]BCPP-EF  $V_T$  between PD patients at follow-up compared with baseline (Table 3, Table S3). [ $^{18}\text{F}$ ]BCPP-EF  $f_p$  was higher in PD at follow-up compared with baseline ( $P = 0.049$ ; Table S1); therefore, regional longitudinal analysis was repeated using  $V_T/f_p$  as an outcome measure showing that the results for [ $^{18}\text{F}$ ]BCPP-EF were unaltered (data not shown). There was no difference in  $f_p$  imaging Data Analysis for [ $^{11}\text{C}$ ]UCB-J or [ $^{11}\text{C}$ ]SA-4503 in PD patients at follow-up compared with baseline (Table S1).

### MRI Volumetric Analysis

FreeSurfer analysis showed no cross-sectional or longitudinal differences in cortical thickness or subcortical volumes. Volumetric analysis of the substantia nigra revealed loss of volume in early drug-naïve PD, whereas no volumetric differences were observed in the locus coeruleus compared with healthy controls (Table S4).

## Discussion

Our preliminary findings indicate the presence of SV2A synaptic loss in the striatum, thalamus, dorsal raphe nuclei, brain stem, and cortical regions at the early

symptomatic stages of PD, with SV2A loss in the brain stem associated with the severity of motor symptoms and total disease burden. In early drug-naïve PD patients, lower levels of  $\sigma 1\text{R}$  and MC1 were observed but with no significant changes. Larger in vivo human studies may provide further understanding into the role of  $\sigma 1\text{R}$  and MC1 in the pathophysiology of PD. Longitudinal analyses revealed the highest annualized reduction of SV2A in the caudate, whereas  $\sigma 1\text{R}$  and MC1 showed the highest annualized increases in the caudate and putamen, respectively, but not reaching statistical significance.

Preclinical studies have demonstrated that the accumulation of  $\alpha$ -synuclein in presynaptic terminals is linked to disruption of synaptic proteins, impaired synaptic plasticity, altered dopaminergic neurotransmission, and loss of striatal dopaminergic neurons.<sup>48</sup> Postmortem studies have shown  $\alpha$ -synuclein aggregates located in synaptosomal protein extracts and that  $\alpha$ -synuclein pathology prominently involves synaptic compartments.<sup>3</sup> Moreover, early synaptic dysfunction because of  $\alpha$ -synuclein presynaptic deposition results in axonal damage.<sup>7,8,16</sup> It has been hypothesized that  $\alpha$ -synuclein synaptic deposition is a crucial event inducing the onset of axonal damage and that neurodegenerative mechanisms in PD could occur as a consequence of synaptic/axonal dieback.<sup>49</sup> SV2A is responsible for maintaining a readily releasable pool of synaptic vesicles through the regulation of endocytosis involving synaptic vesicle proteins such as synaptotagmin-1.<sup>50</sup> Therefore, loss of SV2A density could lead to altered synaptic vesicle release, synaptic and subsequent axonal damage, and increasing accumulation of connectome dysfunction, which may have relevance to the development of PD symptoms. Our findings indicate the presence of SV2A pathology in early drug-naïve PD patients with the highest degree of SV2A loss corresponding to regions known to be affected early in the spread of  $\alpha$ -synuclein pathology.<sup>51</sup> Furthermore, striatal SV2A loss is consistent with presynaptic dopaminergic damage of the nigrostriatal pathway, measured with in vivo dopaminergic imaging including [ $^{123}\text{I}$ ]FP-CIT SPECT, [ $^{11}\text{C}$ ]PE2I, and [ $^{11}\text{C}$ ]DTBZ PET.<sup>52</sup>

In early drug-naïve PD patients, we observed nonsignificant lower levels of  $\sigma 1\text{R}$  and MC1, with the greatest effect size in the caudate and the dorsal raphe, respectively. Our results did not reach statistical significance in this pilot cohort, possibly because of small sample size and early disease stage. The lack of significant findings in early PD could indicate that  $\sigma 1\text{R}$  and MC1 pathology plays a more prominent role in more advanced disease stages.<sup>53-56</sup> However, further studies in larger cohorts of early drug-naïve and in moderate-advanced PD, as well as in familial forms of PD, are warranted to fully elucidate the role of mitochondrial-ER dysfunction in disease pathophysiology.

Exploratory analysis investigating the relationship between SV2A,  $\sigma 1\text{R}$ , and MC1 at a molecular level

showed preliminary indications for the concurrent and colocalized loss of SV2A,  $\sigma$ 1R, and MC1 in the caudate and brain stem regions in drug-naïve PD patients. These findings suggest a potential pathophysiological interplay between mitochondrial adenosine triphosphate production, control of  $\text{Ca}^{2+}$  influx from the ER into the mitochondria and synaptic function at early PD stages. However, because we did not find significant cross-sectional changes in  $\sigma$ 1R and MC1, these preliminary findings should be interrupted with caution. The precise sequence of events for synaptic pathology and mitochondrial and  $\sigma$ 1R dysfunction in the neurodegenerative process underlying the onset and progression of PD remains unclear. There are hypotheses on the pathways linking the accumulation of presynaptic  $\alpha$ -synuclein pathology resulting in mitochondrial damage and vice versa.<sup>57</sup> Further work is warranted to confirm these findings and to better understand the exact timing of such mechanistic changes to help identify the earliest changes for potential therapeutic interventions.

In our longitudinal analysis, nonsignificant annualized SV2A loss was greatest in the caudate, with widespread nonsignificant annualized increases of  $\sigma$ 1R and MC1 that were highest in the caudate and putamen, respectively. Because of the small longitudinal changes in SV2A, we cannot fully exclude the possibility that the longitudinal changes observed reflect, at least in part, tracer test–retest variability.<sup>44</sup> Given that the longitudinal analysis in this cohort did not show any significant results, we cannot draw any firm conclusions. However, some preclinical evidence indicates that increased levels of  $\sigma$ 1R could represent a potential neuroprotective effect to promote neuronal survival, prevent the accumulation of abnormal proteins, and promote mitochondrial functions.<sup>19,20,58,59</sup> The possible interactions between synaptic and mitochondrial-ER molecular components and pathways in PD progression warrant further investigation.

We also evaluated [<sup>11</sup>C]UCB-J DVR-1 as an outcome measure, which is equivalent to [<sup>11</sup>C]UCB-J BP<sub>ND</sub> previously reported.<sup>44,60,61</sup> Although [<sup>11</sup>C]UCB-J V<sub>T</sub> and [<sup>11</sup>C]UCB-J DVR-1 both showed consistent loss of SV2A, only changes in [<sup>11</sup>C]UCB-J V<sub>T</sub> survived FDR correction for multiple comparisons. As the centrum semiovale contains some displaceable binding,<sup>44</sup> its use as a pseudo-reference region should be conducted with caution, as changes in the binding in the centrum semiovale may mask some of the effects in the target regions. This may explain the differences in our results between [<sup>11</sup>C]UCB-J V<sub>T</sub> and [<sup>11</sup>C]UCB-J DVR-1 analysis. Recently, loss of [<sup>11</sup>C]UCB-J BP<sub>ND</sub> has been reported in the substantia nigra, red nucleus, and locus coeruleus in moderate to advanced PD patients, with autoradiography also showing SV2A loss in the substantia nigra.<sup>61</sup> Taking our findings together with the findings from Matuskey and colleagues indicates that synaptic density loss could start early in disease pathophysiology,

with more pronounced loss in moderate to advanced stages. However, our longitudinal analysis suggests that the annual rate of SV2A decline is likely to be slow, at least in early disease stages. The lack of significant findings in the longitudinal evaluation is likely because of the small sample size, the relatively short follow-up period, and the very early disease stage of the PD patients. The 1-year follow-up period was chosen in line with the need to identify sensitive readouts that can track early disease progression and could have the potential as measures of therapeutic response in future clinical trials. Volumetric analysis revealed loss of volume only in the substantia nigra (–26%) in early drug-naïve PD patients compared with healthy controls. Therefore, we cannot fully exclude the possible effect of volume loss on PET measures in the substantia nigra and that the changes observed in SV2A,  $\sigma$ 1R, and MC1 within the substantia nigra do not reflect, at least in part, neuronal loss.

In summary, this is the first study to show *in vivo* evidence for changes in synaptic density in a cohort of very early drug-naïve PD patients. We found prominent loss of SV2A presynaptic density in early stages of PD, which may be promoted by  $\alpha$ -synuclein pathology and have relevance to symptomatology. Therefore, the development of new therapies focusing on the regeneration of synapses, moving away from solely the restoration of extracellular dopamine levels, may represent a novel therapeutic mechanism with a potentially earlier therapeutic window aimed at the preservation and restoration of synaptic function prior to neuronal damage and loss in PD. Further *in vivo* studies with larger cohorts and longer follow-up periods are warranted to fully elucidate the role of SV2A, MC1, and  $\sigma$ 1R dysfunction in the pathophysiology and symptomatology of PD and to validate [<sup>11</sup>C]UCB-J, [<sup>11</sup>C]SA-4503, and [<sup>18</sup>F]BCPP-EF PET as potential markers to track disease progression in moderate-advanced stages of PD. ■

**Acknowledgments:** We thank all participants and their families, the radiochemists, PET technicians, MRI radiographers, and the clinical research nurses at Invicro (London, UK) for their excellent technical support. Thank you to the team at the NIHR King's Wellcome Clinical Research Facility. Special thanks to Ms. Tayyabah Yousaf at the Neurodegeneration Imaging Group, King's College London (London, UK). This study was performed as part of the Molecular Imaging in NeuroDegeneration – Mitochondria, Associated Proteins & Synapses (MIND-MAPS) programme (<http://www.invicro.com/mindmaps>), with the input and support of the MIND-MAPS consortium members: Laurent Martarello, Biogen; Robert A. Comley, AbbVie; Laigao Chen, Pfizer; Adam Schwarz, Takeda; Hideo Tsukada, Hamamatsu Photonics; Paul Matthews, Imperial College London; Jonathan Rohrer, University College London; David Brooks, Newcastle University; James B. Rowe, University of Cambridge. MIND-MAPS is a precompetitive industry and academia consortium that aims to investigate the utility of these markers of mitochondrial/ER/synapse axis to monitor the progress of neurodegeneration across neurodegenerative disorders. The healthy volunteer data were provided by a cohort collected by the MIND-MAPS consortium. Dr Silvia Paola Caminiti was supported by Parkinson's Foundation Vising Scholar Award (PF-VSA-SFW-1824). Professor Marios Politis research is supported by Michael J. Fox Foundation for Parkinson's Research, Edmond and Lilly Safra Foundation, CHDI Foundation, Glaxo Wellcome R&D, Life Molecular Imaging, Invicro, Curium, Medical Research Council (UK), AVID Radiopharmaceuticals, National Institute for Health

Research, Alzheimer's Research UK, and European Commission IMI2 fund.

## Author Contributions

M.P. conceived the study, conceptualized the experimental design and acquired funding for the study. G.P. and E.D.N. performed the imaging and clinical assessments. G.P., S.P., E.A.R., and M.P. organized the study. G.P., E.D.N., S.P., L.T.M., and G.Pr. recruited the participants. H.W. wrote the first draft, generated the figures, and prepared the article. H.W., G.P., S.P.C., and A.M. analyzed the data. M.P., H.W., G.P., A.M., R.N.G., K.F.S., and E.A.R. interpreted the data. All authors revised and gave input to the article.

## Data Availability Statement

The authors confirm that the data supporting the findings of this study are available within the article and its supplementary material.

## References

- Park JS, Davis RL, Sue CM. Mitochondrial Dysfunction in Parkinson's Disease: New mechanistic insights and therapeutic perspectives. *Curr Neurol Neurosci Rep* 2018;18(5):21.
- Colla E. Linking the endoplasmic reticulum to Parkinson's disease and alpha-synucleinopathy. *Front Neurosci* 2019;13:560.
- Schulz-Schaeffer WJ. The synaptic pathology of alpha-synuclein aggregation in dementia with Lewy bodies, Parkinson's disease and Parkinson's disease dementia. *Acta Neuropathol* 2010;120(2):131–143.
- Bajjalieh SM, Peterson K, Shinghal R, Scheller RH. SV2, a brain synaptic vesicle protein homologous to bacterial transporters. *Science* 1992;257(5074):1271–1273.
- Vogl C, Tanifuji S, Danis B, Daniels V, Foerch P, Wolff C, et al. Synaptic vesicle glycoprotein 2A modulates vesicular release and calcium channel function at peripheral sympathetic synapses. *Eur J Neurosci* 2015;41(4):398–409.
- Cohen JE, Lee PR, Chen S, Li W, Fields RD. MicroRNA regulation of homeostatic synaptic plasticity. *Proc Natl Acad Sci U S A* 2011;108(28):11650–11655.
- Bellucci A, Zaltieri M, Navarra L, Grigoletto J, Missale C, Spano P. From alpha-synuclein to synaptic dysfunctions: new insights into the pathophysiology of Parkinson's disease. *Brain Res* 2012;1476:183–202.
- Anichtchik O, Calo L, Spillantini MG. Synaptic dysfunction in synucleinopathies. *CNS Neurol Disord Drug Targets* 2013;12(8):1094–1100.
- Ben Gedalya T, Loeb V, Israeli E, Altschuler Y, Selkoe DJ, Sharon R. Alpha-synuclein and polyunsaturated fatty acids promote clathrin-mediated endocytosis and synaptic vesicle recycling. *Traffic* 2009;10(2):218–234.
- Nemani VM, Lu W, Berge V, et al. Increased expression of alpha-synuclein reduces neurotransmitter release by inhibiting synaptic vesicle reclustering after endocytosis. *Neuron* 2010;65(1):66–79.
- Cheng F, Vivacqua G, Yu S. The role of alpha-synuclein in neurotransmission and synaptic plasticity. *J Chem Neuroanat* 2011;42(4):242–248.
- Vargas KJ, Makani S, Davis T, Westphal CH, Castillo PE, Chandra SS. Synucleins regulate the kinetics of synaptic vesicle endocytosis. *J Neurosci* 2014;34(28):9364–9376.
- Burre J, Vivona S, Diao J, Sharma M, Brunger AT, Sudhof TC. Properties of native brain alpha-synuclein. *Nature* 2013;498(7453):E4–E6; discussion E-7.
- Lai Y, Kim S, Varkey J, et al. Nonaggregated alpha-synuclein influences SNARE-dependent vesicle docking via membrane binding. *Biochemistry* 2014;53(24):3889–3896.
- Choi BK, Kim JY, Cha MY, Mook-Jung I, Shin YK, Lee NK. beta-Amyloid and alpha-synuclein cooperate to block SNARE-dependent vesicle fusion. *Biochemistry* 2015;54(9):1831–1840.
- Hunn BH, Cragg SJ, Bolam JP, Spillantini MG, Wade-Martins R. Impaired intracellular trafficking defines early Parkinson's disease. *Trends Neurosci* 2015;38(3):178–188.
- Mavlyutov TA, Guo LW, Epstein ML, Ruoho AE. Role of the Sigma-1 receptor in Amyotrophic Lateral Sclerosis (ALS). *J Pharmacol Sci* 2015;127(1):10–16.
- Tsai SY, Pokrass MJ, Klauer NR, De Credico NE, Su TP. Sigma-1 receptor chaperones in neurodegenerative and psychiatric disorders. *Expert Opin Ther Targets* 2014;18(12):1461–1476.
- Hayashi T, Su TP. Sigma-1 receptor chaperones at the ER-mitochondrion interface regulate Ca(2+) signaling and cell survival. *Cell* 2007;131(3):596–610.
- Renaudo A, L'Hoste S, Guizouarn H, Borgese F, Soriani O. Cancer cell cycle modulated by a functional coupling between sigma-1 receptors and Cl- channels. *J Biol Chem* 2007;282(4):2259–2267.
- Booth RG, Baldessarini RJ. (+)-6,7-benzomorphan sigma ligands stimulate dopamine synthesis in rat corpus striatum tissue. *Brain Res* 1991;557(1–2):349–352.
- Papa S, De Rasmio D. Complex I deficiencies in neurological disorders. *Trends Mol Med* 2013;19(1):61–69.
- Ryan BJ, Hoek S, Fon EA, Wade-Martins R. Mitochondrial dysfunction and mitophagy in Parkinson's: from familial to sporadic disease. *Trends Biochem Sci* 2015;40(4):200–210.
- Moon HE, Paek SH. Mitochondrial Dysfunction in Parkinson's Disease. *Exp Neurobiol* 2015;24(2):103–116.
- Flores IH, Fernandez-Vizarrá E, Lykouri M, et al. Neuronal complex I deficiency occurs throughout the Parkinson's disease brain, but is not associated with neurodegeneration or mitochondrial DNA damage. *Acta Neuropathol* 2018;135(3):409–425.
- Schapira AH. Mitochondrial complex I deficiency in Parkinson's disease. *Adv Neurol* 1993;60:288–291.
- Schapira AH, Cooper JM, Dexter D, Clark JB, Jenner P, Marsden CD. Mitochondrial complex I deficiency in Parkinson's disease. *J Neurochem* 1990;54(3):823–827.
- Schapira AH, Cooper JM, Dexter D, Jenner P, Clark JB, Marsden CD. Mitochondrial complex I deficiency in Parkinson's disease. *Lancet* 1989;1(8649):1269.
- Nabulsi NB, Mercier J, Holden D, et al. Synthesis and Preclinical Evaluation of <sup>11</sup>C-UCB-J as a PET tracer for imaging the synaptic vesicle glycoprotein 2A in the Brain. *J Nucl Med* 2016;57(5):777–784.
- Ogawa K, Masuda R, Mizuno Y, et al. Development of a novel radiobromine-labeled sigma-1 receptor imaging probe. *Nucl Med Biol* 2018;61:28–35.
- Kazami S, Nishiyama S, Kimura Y, Itoh H, Tsukada H. BCPP compounds, PET probes for early therapeutic evaluations, specifically bind to mitochondrial complex I. *Mitochondrion* 2019;46:97–102.
- Toyohara J, Kobayashi T, Mita S, Ishiwata K. Application of [(1)(1)C]SA4503 to selection of novel sigma(1) selective agonists. *Nucl Med Biol* 2012;39(8):1117–121.
- Litvan I, Aarsland D, Adler CH, et al. MDS Task Force on mild cognitive impairment in Parkinson's disease: critical review of PD-MCI. *Mov Disord* 2011;26(10):1814–1824.
- Emre M, Aarsland D, Brown R, et al. Clinical diagnostic criteria for dementia associated with Parkinson's disease. *Mov Disord* 2007;22(12):1689–1707; quiz 837.
- Marsh L, McDonald WM, Cummings J, Ravina B; NINDS/NIMH Work Group on Depression and Parkinson's Disease. Provisional diagnostic criteria for depression in Parkinson's disease: report of an NINDS/NIMH Work Group. *Mov Disord* 2006;21(2):148–158.

36. Sudhyadhom A, Haq IU, Foote KD, Okun MS, Bova FJ. A high resolution and high contrast MRI for differentiation of subcortical structures for DBS targeting: the Fast Gray Matter Acquisition T1 Inversion Recovery (FGATIR). *Neuroimage* 2009;47(Suppl 2):T44–T52.
37. Fischl B, Salat DH, Busa E, et al. Whole brain segmentation: automated labeling of neuroanatomical structures in the human brain. *Neuron* 2002;33(3):341–355.
38. Malone IB, Leung KK, Clegg S, et al. Accurate automatic estimation of total intracranial volume: a nuisance variable with less nuisance. *Neuroimage* 2015;104:366–372.
39. Tziortzi AC, Searle GE, Tzimopoulou S, et al. Imaging dopamine receptors in humans with C-11 -(+)-PHNO: dissection of D3 signal and anatomy. *Neuroimage* 2011;54(1):264–277.
40. Mansur A, Rabiner EA, Comley RA, et al. Characterization of 3 PET tracers for quantification of mitochondrial and synaptic function in healthy human brain: (18)F-BCPP-EF, (11)C-SA-4503, (11)C-UCB-J. *J Nucl Med* 2020;61(1):96–103.
41. Ichise M, Toyama H, Innis RB, Carson RE. Strategies to improve neuroreceptor parameter estimation by linear regression analysis. *J Cereb Blood Flow Metab* 2002;22(10):1271–1281.
42. Logan J, Fowler JS, Volkow ND, et al. Graphical analysis of reversible radioligand binding from time-activity measurements applied to [N-11C-methyl]-(-)-cocaine PET studies in human subjects. *J Cereb Blood Flow Metab* 1990;10(5):740–747.
43. Gunn RN, Gunn SR, Cunningham VJ. Positron emission tomography compartmental models. *J Cereb Blood Flow Metab* 2001;21(6):635–652.
44. Finnema SJ, Nabulsi NB, Mercier J, et al. Kinetic evaluation and test-retest reproducibility of [(11)C]UCB-J, a novel radioligand for positron emission tomography imaging of synaptic vesicle glycoprotein 2A in humans. *J Cereb Blood Flow Metab* 2018;38(11):2041–2052.
45. Edlow BL, Takahashi E, Wu O, et al. Neuroanatomic connectivity of the human ascending arousal system critical to consciousness and its disorders. *J Neuropathol Exp Neurol* 2012;71(6):531–546.
46. Ishiwata K, Kobayashi T, Kawamura K, Matsuno K. Age-related changes of the binding of [3h]SA4503 to sigma1 receptors in the rat brain. *Ann Nucl Med* 2003;17(1):73–77.
47. Benjamini Y, Cohen R. Weighted false discovery rate controlling procedures for clinical trials. *Biostatistics* 2017;18(1):91–104.
48. Bellucci A, Mercuri NB, Venneri A, et al. Review: Parkinson's disease: from synaptic loss to connectome dysfunction. *Neuropathol Appl Neurobiol* 2016;42(1):77–94.
49. Calo L, Wegrzynowicz M, Santivaney-Perez J, Grazia Spillantini M. Synaptic failure and alpha-synuclein. *Mov Disord* 2016;31(2):169–177.
50. Yao J, Nowack A, Kensel-Hammes P, Gardner RG, Bajjalieh SM. Cotrafficking of SV2 and synaptotagmin at the synapse. *J Neurosci* 2010;30(16):5569–5578.
51. Braak H, Del Tredici K, Rub U, de Vos RA, Jansen Steur EN, Braak E. Staging of brain pathology related to sporadic Parkinson's disease. *Neurobiol Aging* 2003;24(2):197–211.
52. Politis M. Neuroimaging in Parkinson disease: from research setting to clinical practice. *Nat Rev Neurol* 2014;10(12):708–722.
53. Toyohara J, Sakata M, Ishiwata K. Imaging of sigma1 receptors in the human brain using PET and [11C]SA4503. *Cent Nerv Syst Agents Med Chem* 2009;9(3):190–196.
54. Mishina M, Ishiwata K, Ishii K, et al. Function of sigma1 receptors in Parkinson's disease. *Acta Neurol Scand* 2005;112(2):103–107.
55. Keeney PM, Xie J, Capaldi RA, Bennett JP Jr. Parkinson's disease brain mitochondrial complex I has oxidatively damaged subunits and is functionally impaired and misassembled. *J Neurosci* 2006;26(19):5256–5264.
56. Kanazawa M, Ohba H, Nishiyama S, Kakiuchi T, Tsukada H. Effect of MPTP on serotonergic neuronal systems and mitochondrial complex I activity in the living brain: a pet study on conscious rhesus monkeys. *J Nucl Med* 2017;58(7):1111–1116.
57. Zaltieri M, Longhena F, Pizzi M, Missale C, Spano P, Bellucci A. Mitochondrial dysfunction and alpha-synuclein synaptic pathology in Parkinson's disease: who's on first? *Parkinsons Dis* 2015;2015:108029.
58. Gogvadze N, Zhuravliova E, Morin D, Mikeladze D, Maurice T. Sigma-1 receptor agonists induce oxidative stress in mitochondria and enhance complex I activity in physiological condition but protect against pathological oxidative stress. *Neurotox Res* 2019;35(1):1–18.
59. Francardo V, Bez F, Wieloch T, Nissbrandt H, Ruscher K, Cenci MA. Pharmacological stimulation of sigma-1 receptors has neurorestorative effects in experimental parkinsonism. *Brain* 2014;137(Pt 7):1998–2014.
60. Chen MK, Mecca AP, Naganawa M, et al. Assessing synaptic density in Alzheimer disease with synaptic vesicle glycoprotein 2A positron emission tomographic imaging. *JAMA Neurol* 2018;75(10):1215–1224.
61. Matuskey D, Tinaz S, Wilcox KC, et al. Synaptic changes in Parkinson's disease assessed with in-vivo imaging. *Ann Neurol* 2020;87(#):329–338.

## Supporting Data

Additional Supporting Information may be found in the online version of this article at the publisher's web-site.